205.8Tb/s Weakly-Coupled 2-Mode 7-Core Transmission Over 1170-km FM-MCF Only Using 2×2 MIMO-DSP

Gang Qiao[1], Yu Yang[2], Honglin Ji[2], Shuailuo Huang[1], Chengbin Long[1], Yuyang Gao[1], Mingqing Zuo[1], Jiarui Zhang[1], Zhaopeng Xu[2], Qi Wu[2], Shangcheng Wang[2], Lulu Liu[2], Lei Shen[3], Jie Luo[3], Junpeng Liang[2], Zhixue He[2], Yongqi He[1], Weisheng Hu[2], Zhangyuan Chen[1], Juhao Li[1,2*]

[1]*State Key Laboratory of Advanced Optical Communication Systems and Networks, Peking University, Beijing 100871, China.*
[2]*Peng Cheng Laboratory, Shenzhen, 518055, China*
[3]*State Key Laboratory of Optical Fiber and Cable Manufacture Technology, YOFC, Wuhan, China.*
juhao_li@pku.edu.cn

Abstract: We demonstrate the first long-haul weakly-coupled FM-MCF transmission adopting non-degenerate LP_{01} and LP_{02} modes in a 6-LP-mode 7-core fiber. 205.8Tb/s throughput over 1170 km transmission with DP-QPSK modulation is achieved only utilizing 2×2 MIMO-DSP. © 2024 The Author(s)

1. Introduction

Space division multiplexing (SDM) techniques based on few-mode fibers (FMF), multicore fibers (MCF) and few-mode multicore fibers (FM-MCF) have been extensively investigated to meet the ever-increasing demand for ultra-broadband optical communications systems [1-3]. Although long-haul strongly-coupled SDM transmissions have been successfully demonstrated [4], the huge computation complexity of inter-mode or inter-core multiple-input multiple-output digital signal processing (MIMO-DSP) may greatly impede their practical implementation [5]. Weakly-coupled SDM transmission by transmitting/receiving light in different linearly-polarized (LP) modes or cores independently without inter-channel MIMO-DSP has attracted great interest, in which crosstalk among different cores and modes in the whole link including transmission fiber, fan-in/fan-out (FI/FO) devices, mode multiplexers/demultiplexer (MMUX/MDEMUX) and other components should be suppressed as much as possible [6]. In our recent study, the required level of distributed modal crosstalk to support long-haul weakly-coupled mode-division-multiplexing (MDM) transmission has been analyzed, and the feasibility of weakly-coupled long-haul MDM and wavelength division multiplexing (WDM) transmission with up to 4×4 MIMO-DSP has been experimentally demonstrated [7]. In this paper, we extend it to the case of weakly-coupled FM-MCF transmission. A weakly-coupled 6-LP-mode 7-core fiber is first designed and fabricated. The matched FI/FO devices are fabricated by fiber bundling processing, and the matched MMUX/MDEMUX consisting of cascaded mode-selective couplers (MSCs) are realized, both of which achieve low insertion loss and crosstalk. Based on the proposed FM-MCF and optical components, we successfully demonstrate 1170-km weakly-coupled SDM-WDM loop transmission only utilizing 2×2 MIMO-DSP, for which a total throughput of 205.8Tb/s is achieved across C-band with dual-polarization quadrature phase shift keying (DP-QPSK) modulation.

2. Weakly-coupled transmission FM-MCF and matched spatial MUX/DEMUX

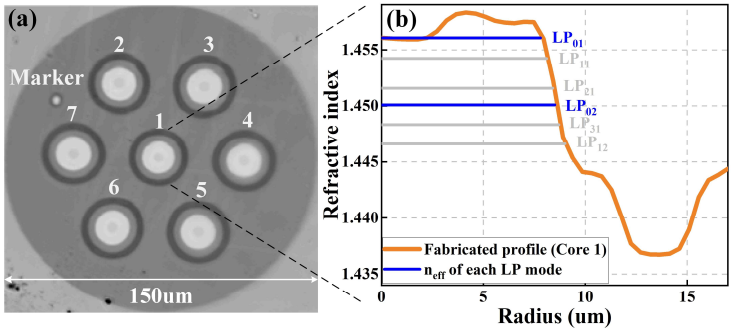

Fig. 1 (a) Picture of fiber cross-section. (b) Index profile of Core 1.

Table 1 Characteristics of non-degenerate modes in the weakly-coupled FM-MCF.

	LP_{01}	LP_{02}
n_{eff}	1.456	1.450
Δn_{eff} ($\times 10^{-3}$)	6	--
A_{eff} (um^2)	150	121
CD* (ps/nm·km)	20	25.5
PL** (dB/km)	0.215	0.232

*CD: chromatic dispersion **PL: propagation loss

Figure 1(a) shows the picture of cross-section of the fabricated 6-mode 7-core fiber with cladding diameter of 150 μm and pitch of 42 μm. Fig. 1(b) illustrates the index profile of the few-mode Core 1 and effective refractive index n_{eff}

distribution of six supported LP modes (LP_{01} to LP_{12}). To suppress inter-modal crosstalk, index perturbation rings are applied in the cores to greatly enhance the minimum n_{eff} difference among LP modes [8]. Trenches are utilized around the cores to suppress the inter-core crosstalk and reduce the bending loss of high-order LP modes. We only choose the two non-degenerate LP_{01} and LP_{02} modes as the transmission channels because they are highly compatible with conventional single-mode transceivers with simple 2×2 MIMO-DSP. Characteristics of the two non-degenerate modes at 1550 nm are listed in Table 1. The large Δn_{eff} of 6×10^{-3} means that the distributed modal crosstalk between them could be low enough to support long-haul weakly-coupled MDM transmission. The measured inter-core crosstalk is lower than -60 dB for both LP_{01} and LP_{02} modes.

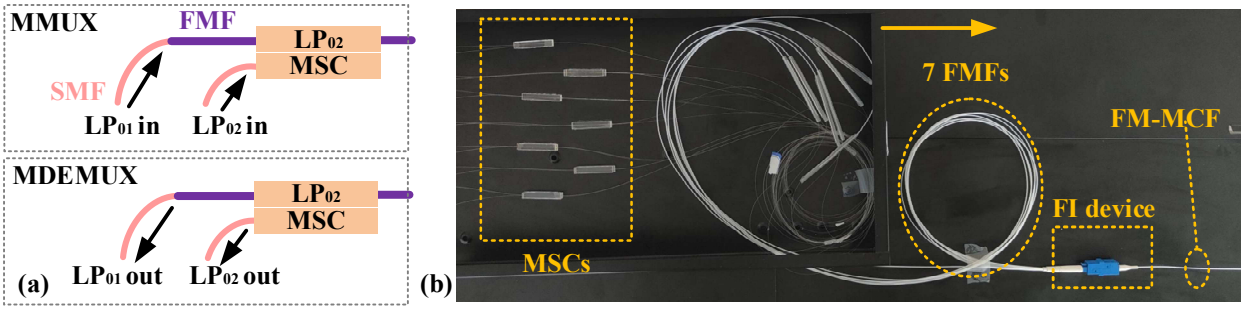

Fig. 2 (a) Cascaded structure of the MMUX/MDEMUX. (b) Picture of the spatial MUX.

The schematic diagram of the spatial multiplexer/demultiplexer (MUX/DEMUX) for FM-MCF transmission is shown in Fig. 2. Mode-selective couplers (MSC) are utilized to convert light from the fundamental mode of SMF into the LP_{02} mode in the FMF, and vice versa, as shown in Fig. 2(a). The MSCs are fabricated by side polishing and mating process to reduce the insertion loss and modal crosstalk [9]. Center alignment method is adopted for the excitation of LP_{01} mode at the FMF input port of the MSCs. The fiber-bundle-type FI/FO devices are fabricated by gathering seven thin-cladding FMFs into a sleeve. The cores of the seven thin-cladding FMFs are hexagonally arrayed and their relative positions correspond to each core of the FM-MCF. To minimize extra insertion loss and modal crosstalk caused by the mode field mismatching at butt coupling, the FMF cores of MMUM/MDEMUX, FI/FO devices and the FM-MCF are designed to be essentially identical. The picture of the spatial MUX consists of 7 sets of MMUXes and an FI device is shown in Fig. 2(b). The back-to-back (B2B) inter-core crosstalk among all the seven cores is measured to be less than -55 dB. The worst intra-core modal crosstalk and insertion loss of the B2B spatial MUX/DEMUX are -25.9 dB and -1.2 dB, respectively.

3. Experimental setup and result

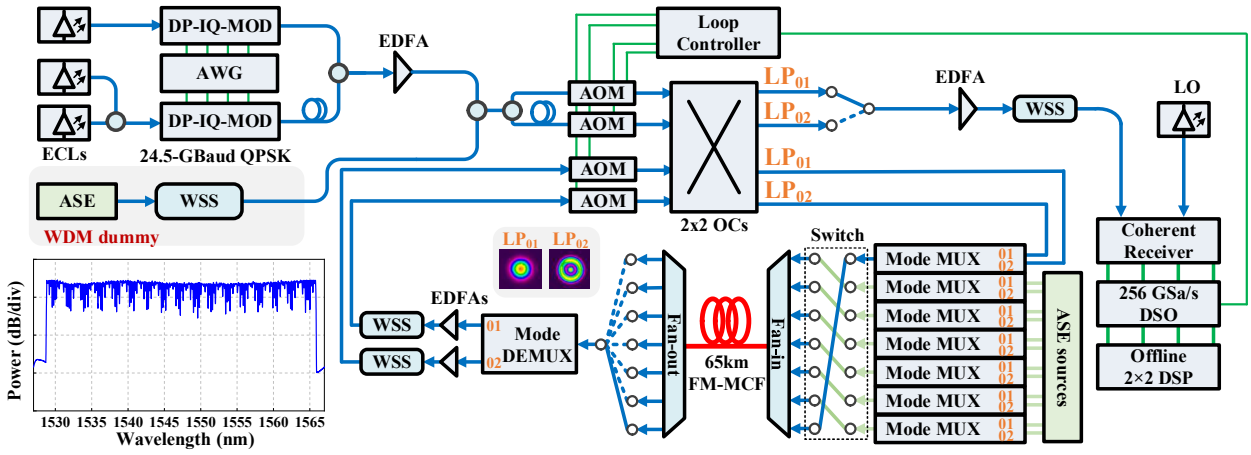

Fig. 3 Experimental setup for the 1170-km recirculating-loop FM-MCF transmission.

The experimental setup for 1170-km 2-mode 7-core SDM transmission is shown in Fig. 3. At the transmitter, three optical carriers are generated by external-cavity lasers (ECL, IDPHOTONES CBMA48). For the test channel, an arbitrary waveform generator (AWG, Keysight M8199A) operating at 128 GSa/s is employed to generate 24.5-GBaud Nyquist-shaped quadrature phase shift keying (QPSK) baseband signal with a roll-off factor of 0.01, which drives a dual-polarization in-phase and quadrature modulator (DP-IQ-MOD). Two neighboring channels are generated with the same method and are de-corrected with 50-ns delay. Wavelength-division multiplexing (WDM) dummy channels

are created using an amplified spontaneous emission (ASE) source followed by a wavelength-selective switch (WSS, Finisar WaveShaper 400A). The WSS filters the optical spectrum to add guard intervals and make a notch to accommodate the test channel and the neighboring channels. Thus, all the combined signals could emulate 180-channel WDM spectrum over the C-band (1529.8~1565.1 nm) with a channel spacing of 25 GHz, as shown in the inset of Fig. 3. To work through all 180 WDM channels, each time the wavelength of the test channel is tuned, the wavelengths of the two neighbor channels are also tuned to be adjacent, and the filtering shape of the WSS is adjusted to avoid overlap in the optical spectrum. The signal is then split into two paths with relative delay of 150 ns and fed into the recirculating loop for both LP modes.

The recirculating-loop system is composed of a loop controller, four acousto-optic modulators (AOM) and two 2×2 optical couplers (OC). Each transmission span consists of 65-km FM-MCF, a pair of spatial MUX/DEMUX, two EDFAs and two WSSes. The EDFAs are used to compensate for transmission loss, while the WSSes are used for gain flattening. Two sets of 180-channel signals are multiplexed by one of the seven MMUXes and then are fed into the loop by the FI device, while 12 branches of C-band ASE noise are fed into the other six MUXes to fill up all the other spatial channels. The performance of all the seven cores are measured in turns by switching the output ports of the MMUXes. At the receiver, the signal from either of the two non-degenerate modes is amplified by an EDFA and then filtered by another WSS. After the coherent detection, the real-time digital storage oscilloscope (DSO, Keysight UXR0594AP) operating at 256 GSa/s is triggered by the loop controller to capture the signals after specific numbers of loop transmission. Finally, offline 2×2 MIMO-DSP is performed to calculate the performance.

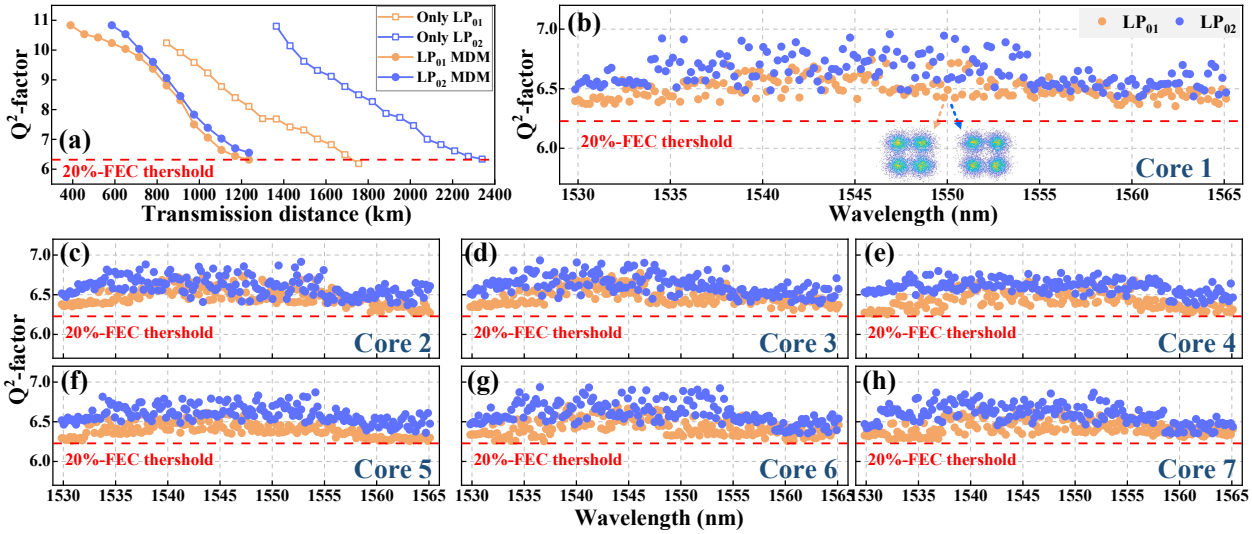

Fig. 4 (a) Q^2-factor versus different transmission distances at 1550 nm. (b)-(h) Q^2-factor for 180 WDM channels of LP_{01} and LP_{02} in each core.

Figure 4(a) shows the Q^2-factor calculated from the measured bit-error rates (BER) at 1550 nm versus different transmission distances for LP_{01} and LP_{02} in Core 1. The 20%-overhead forward-error-correction (FEC) threshold of 6.25 dB is adopted [10]. In the case of individual-mode transmission, the maximum transmission reaches are 1755 km and 2340 km for the LP_{01} mode and LP_{02} modes, respectively. For the case of simultaneous LP_{01}/LP_{02} MDM transmission, the maximum transmission reach is reduced to 1170 km. Fig. 4(b)-(h) show the Q^2-factors in 7 cores after 1170-km transmission, respectively. The worst Q^2-factor is 6.259 dB for LP_{01} at 1564.9 nm in Core 5. Excluding the 20%-FEC overhead, the achieved net rate is 205.8Tb/s for all the SDM-WDM channels.

4. Conclusion

We have demonstrated long-haul weakly-coupled FM-MCF transmission over 1170-km utilizing non-degenerate LP_{01} and LP_{02} modes in 7 cores. A total net rate of 205.8Tb/s is achieved with 14×180×24.5-GBaud DP-QPSK signals at C-band and only 2×2 MIMO-DSP. *This work is supported in part by NSFC (U20A20160 and 62101009), Pengcheng Zili Project (PCL2023AS2-4) and China Postdoc. Foundation (2022M721740).*

5. References

[1] D. J. Richardson, et al., Nat. Photon. **7**(5), 354–362, 2013.
[2] D. Soma et al., IEEE JLT. **36**(6), 1362-1368, 2018.
[3] G. Rademacher, et al., OFC 2023, Th4A.4.
[4] K. Shibahara, et al., OFC 2020, Th3H.3.
[5] R. Ryf, et al., ECOC 2018, Th3B.1.
[6] H. Wen, et al., ECOC 2017, W.2.F.1.
[7] M. Zuo, et al., Opt. Exp. **30**(4), 5868-5878, 2022.
[8] R. Maruyama, et al., IEEE JLT. **35**(4), 650-657, 2017.
[9] J. Cui, et al., OFC 2023, M4E.5.
[10] C. Li, et al., CLEO 2017, STu3M. 4.